

# MEASUREMENTS OF INCLUSIVE AND EXCLUSIVE PARTICLE PRODUCTION AT ZEUS

*I. Kadenko*

*for the ZEUS Collaboration*

Taras Shevchenko National University of Kyiv Department of Nuclear Physics, Kiev

Charged particle production, scaled momentum distributions of identified particles,  $K_s^0$  and  $\Lambda$ , and charged particles for dijet events have been measured in  $ep$  scattering with the ZEUS detector. The evolution of these distributions with the photon virtuality,  $Q^2$ , are studied in the kinematic region  $10 < Q^2 < 40\,000 \text{ GeV}^2$ . The calculations reproduce the measured distributions reasonably well.

PACS: 13.60.-r

## INTRODUCTION

The formation of hadrons in Quantum Chromodynamics (QCD) can be described as a convolution of parton showering (PS) and hadronisation. Within perturbative QCD (pQCD) PS can be described as long as the energy scale involved is sufficiently above the intrinsic scale of QCD,  $\Lambda_{\text{QCD}}$ . Hadronisation describes the process by which coloured partons become confined in colour-neutral hadrons. It cannot be described within pQCD.

pQCD calculations can be performed using matrix elements up to a certain order in the strong coupling constant,  $\alpha_s$ . Alternatively, a resummation approach can be adopted, such as the modified leading-logarithmic approximation (MLLA) [1], where in addition to the fixed-order matrix elements, a subset of dominant terms of all orders in  $\alpha_s$  are included. In particular, pQCD based on the MLLA can be used to predict the multiplicity and momentum spectra of partons produced within cones centred on the initial parton direction. The MLLA may only be used to describe partons at scales above some minimum cutoff,  $\Lambda_{\text{eff}} > \Lambda_{\text{QCD}}$ . The value of  $\Lambda_{\text{eff}}$  is predicted to be independent of the process considered. The local parton hadron duality (LPHD) [2] hypothesis predicts that charged-hadron distributions should be related to the predicted parton distributions by a constant normalisation scaling factor,  $\kappa_{\text{ch}}$ .

Measurement of scaled momentum distributions,  $x_p = 2P_h/Q = P_h/E_{\text{beam}}$ , for  $e^\pm p$  and  $e^+e^-$  collisions is a good test of QCD.

This paper describes new experimental results for scaled momentum distributions obtained by the ZEUS collaboration.

## 1. CHARGED PARTICLE PRODUCTION IN NEUTRAL CURRENT DIS

Charged particle production has been studied in neutral current  $e^\pm p$  DIS with the ZEUS detector at HERA using an integrated luminosity of  $0.44 \text{ fb}^{-1}$  [3]. Distributions of scaled momenta in the Breit frame are presented for particles in the current fragmentation region.

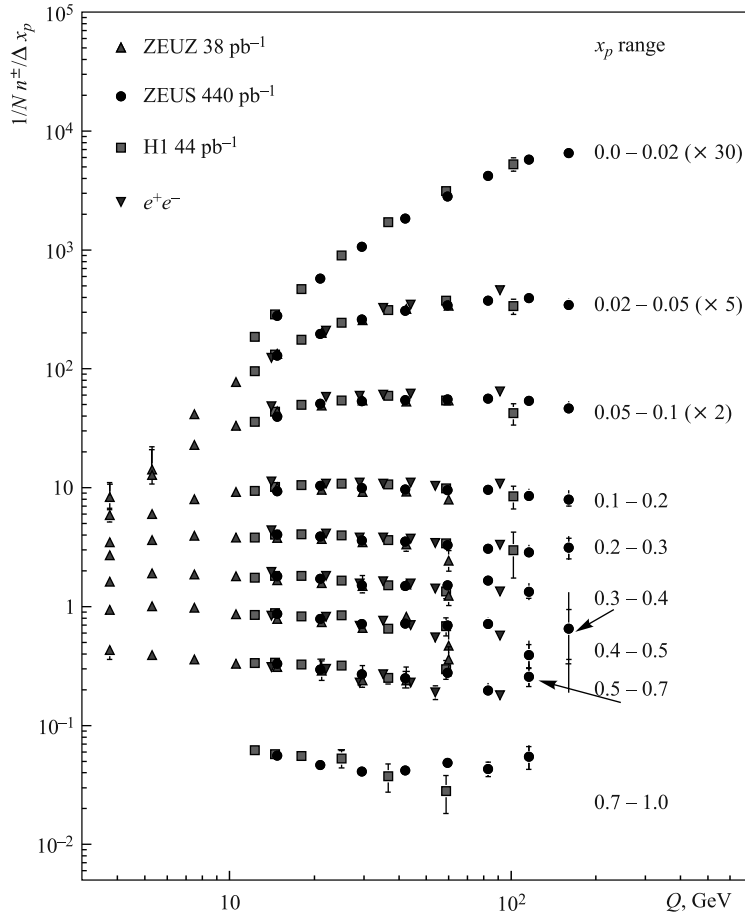


Fig. 1. The number of charged particles per event per unit of  $x_p$ ,  $1/N n^\pm / \Delta x_p$ , as a function of  $Q$  in  $x_p$  bins with width  $\Delta x_p$ . The dots (triangles) represent the new (previous) ZEUS measurement [3, 4], the squares the H1 data [5] and the inverted triangles the  $e^+e^-$  data [6–9]. The three lowest  $x_p$  bins are scaled by factors of 30, 5 and 2, respectively

Figure 1 shows ZEUS [3, 4], H1 [5] results and data from  $e^+e^-$  experiments [6–9]. For a proper comparison, the particle momenta from  $e^+e^-$  data were scaled to half of the centre-of-mass energy and the scale was set to  $Q = 2E_{\text{beam}}$ , where  $E_{\text{beam}}$  is the beam energy. The overall agreement between the different data sets supports fragmentation universality.

Figure 2 shows that the number of charged particles increases with  $Q^2$  at low  $x_p$  and decreases with  $Q^2$  at high  $x_p$ . The predictions from several Monte Carlo (MC) leading-order (LO) QCD models were compared to the measurements. LO QCD Ariadne 4.12 [10] and Lepto 6.5 [11] programs were used. They reproduce the main features of the data but do not

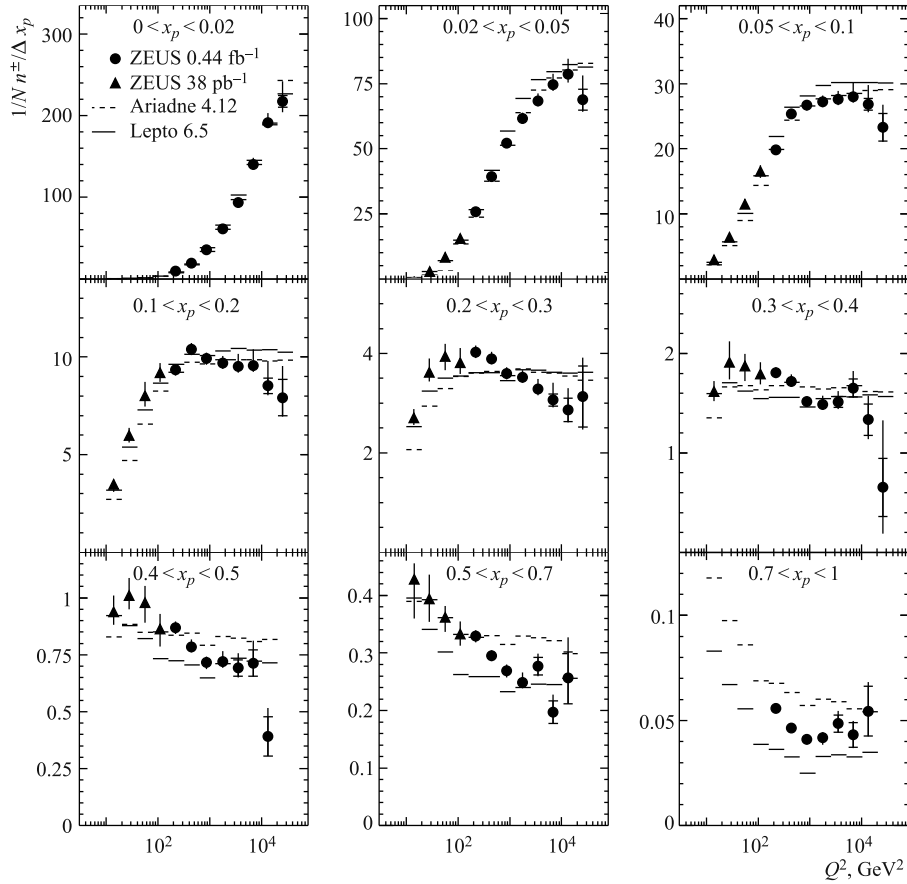


Fig. 2. The number of charged particles per event per unit of  $x_p$ ,  $1/N n^\pm/\Delta x_p$ , as a function of  $Q$  in  $x_p$  bins of width  $\Delta x_p$ . The dots represent the new [3], the triangles the previous ZEUS measurement [4]. The data overlap in the  $160 < Q^2 < 320 \text{ GeV}^2$  bin. The full and dashed lines represent the Lepto [11] and the Ariadne [10] predictions, respectively

agree in detail. For the highest  $Q^2$  bin, both models predict too many charged particles at medium and low values of  $\ln(1/x_p)$ . Lepto also predicts too many particles for medium- $Q^2$  bins, while Ariadne predicts too few for low- $Q^2$  bins. Neither Lepto nor Ariadne provides a good description of this  $Q^2$  dependence over the whole range of  $x_p$ .

Predictions from next-to-leading-order (NLO) QCD calculations that combine full NLO matrix elements are also compared to the measurements. Figure 3 shows the data together with four NLO + FF QCD predictions: Kretzer [12], Kniehl, Kramer, Potter [13] (KKP), Albino, Kniehl, Kramer [14] (AKK) and De Florian, Sassot and Stratmann [15] (DSS) for  $x_p > 0.1$ , where theoretical uncertainties are small and the predictions not too strongly affected by hadron-mass effects which are not included in the calculations. The four predictions are

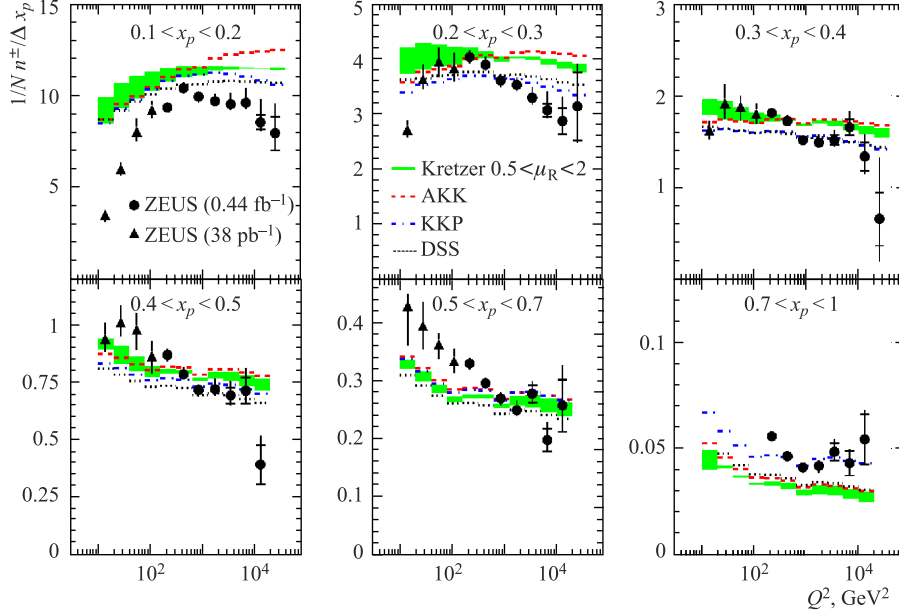


Fig. 3. The number of charged particles per event per unit of  $x_p$ ,  $1/Nn^\pm/\Delta x_p$ , as a function of  $Q$  in  $x_p$  bins of width  $\Delta x_p$ . The shaded band represents the NLO calculation by Kretzer [12] with its renormalisation scale uncertainty. Additional NLO calculations are shown: Kniehl, Kramer, Potter [13] (KKP), Albino, Kniehl, Kramer [14] (AKK) and De Florian, Sassot and Stratmann [15] (DSS)

similar in shape and have similar uncertainties. The NLO calculations also do not provide a good description of the data. Too many particles are predicted at small  $x_p$  and too few at large  $x_p$ . In general, the scaling violations predicted are not strong enough.

## 2. SCALED MOMENTUM DISTRIBUTIONS OF CHARGED PARTICLES FOR DIJET PHOTOPRODUCTION

The multiplicity and scaled momentum distributions of charged hadrons within jets have been measured for dijet photoproduction ( $\gamma p$ ) with the ZEUS detector at HERA using an integrated luminosity of  $359 \text{ pb}^{-1}$  [16]. The events were required to have two and only two reconstructed jets and the sample was enriched in events in which the photon interacted electromagnetically as a point-like particle. The analysis probes energy scales in the range 19 to 38 GeV, which spans the energy region between those accessed previously by the ZEUS, using  $ep$  DIS collisions and CDF collaborations [17]. The distributions are compared to predictions based on pQCD carried out in the framework of the modified MLLA [1] and assuming LPHD [2].

The universal MLLA scale,  $\Lambda_{\text{eff}}$ , and the LPHD parameter,  $\kappa_{\text{ch}}$ , are extracted and their universality tested.

Figure 4 shows the  $\xi = \ln(1/x_p)$  distributions in bins of  $E_{\text{jet}} = M_{2j}/2$  (the hard scale) using different values for opening angles,  $\theta_c$ , around a jet axis. Here  $x_p = p_{\text{track}}/p_{\text{jet}}$

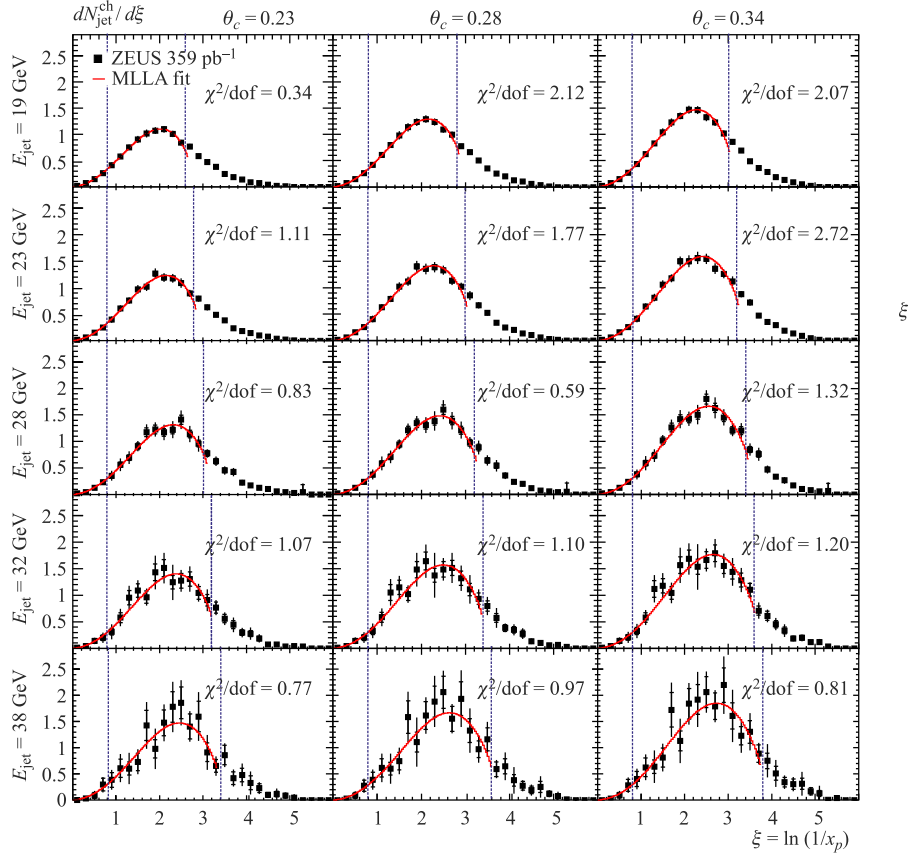


Fig. 4. The  $\xi$  distributions in the five  $E_{\text{jet}}$  bins using the three  $\theta_c$  values. The ZEUS data are shown by solid squares. The limited momentum spectrum predicted by the MLLA (solid line) has been fitted to the data within the regions indicated (dashed lines)

is the measured scaled charge track momentum within jets,  $E_{\text{jet}}$  is the energy of either hadron-level jet in the dijet centre-of-mass frame and  $M_{2j}$  is the invariant dijet mass. The fitted MLLA functions are shown in Fig. 4. While the theory does describe many of the features of the data in the fitting ranges, there are differences. Specifically, the rising edges of the  $\xi$  peaks are well described. However, the upper tails of the distributions are not adequately reproduced. The same was observed in  $e^+e^-$  [18, 19] and  $ep$  DIS [4] data and to a lesser extent in high- $E_{\text{jet}}$   $p\bar{p}$  data [17]. This is likely due to the specific MLLA regularisation scheme used here and in the other aforementioned analysis.

Energy dependence of  $\Lambda_{\text{eff}}$  is shown in Fig. 5. A weak dependence was observed in the CDF data [17], which span a wider range of energy scales. However, the data do suggest that the value of  $\Lambda_{\text{eff}}$  is weakly dependent on  $\theta_c$ . Specifically, Fig. 5 shows that the values of  $\Lambda_{\text{eff}}$

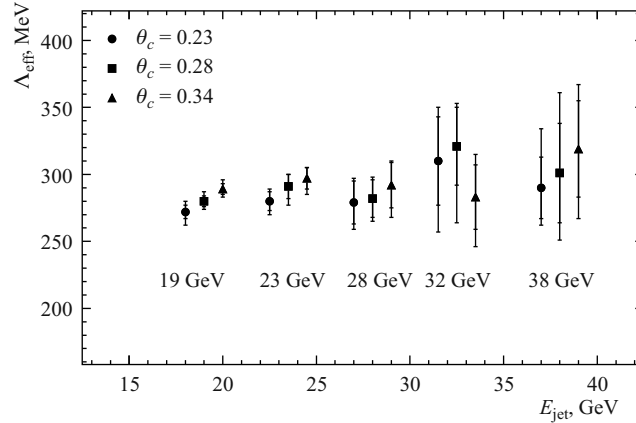


Fig. 5.  $\Lambda_{\text{eff}}$  extracted at the five  $E_{\text{jet}}$  points using the three  $\theta_c$  values. The points have been shifted horizontally for clarity

extracted from the wider cone data tend to be systematically larger. This behaviour was also observed by the CDF collaboration [17].

### 3. SCALED MOMENTUM DISTRIBUTIONS OF IDENTIFIED PARTICLES, $K_s^0$ AND $\Lambda$

Scaled momentum distributions of identified particles,  $K_s^0$  and  $\Lambda$ , have been measured in deep inelastic  $ep$  scattering with the ZEUS detector at HERA using an integrated luminosity of  $290 \text{ pb}^{-1}$  [20]. The evolution of these distributions with the photon virtuality,  $Q^2$ , are studied in the kinematic region  $10 < Q^2 < 40\,000 \text{ GeV}^2$ . The distributions have been measured in the current fragmentation region of the Breit frame.

Scaled momentum distributions for  $K_s^0$  and  $\Lambda$  vs.  $Q^2$  (Fig. 6) show scaling violations. LO QCD Ariadne (CDM) [10] and Lepto (MEPS) [11] calculations describe the data in full phase space. Whereas QCD NLO predictions (AKK [14] and DSS [15]) describe the data in certain regions of the phase space.

Scaled momentum distributions for  $K_s^0$  and  $\Lambda$  vs.  $x_p$  (Fig. 7) show reasonable description by LO Ariadne [10] and Lepto [11] calculations of the data in full phase space. Whereas QCD NLO predictions (AKK [14] and DSS [15]) describe adequately only high- $x_p$  region.

### CONCLUSION

Charged particle spectra have been measured in DIS and photoproduction at HERA. In general, results are found to support the concept of quark fragmentation universality. However, in detail, there exist some issues when comparing the data with theory.

The universal MLLA scale,  $\Lambda_{\text{eff}}$ , and the LPHD parameter,  $\kappa_{\text{ch}}$ , are extracted from scaled momentum distributions of charged particles for dijet photoproduction and their universality tested.

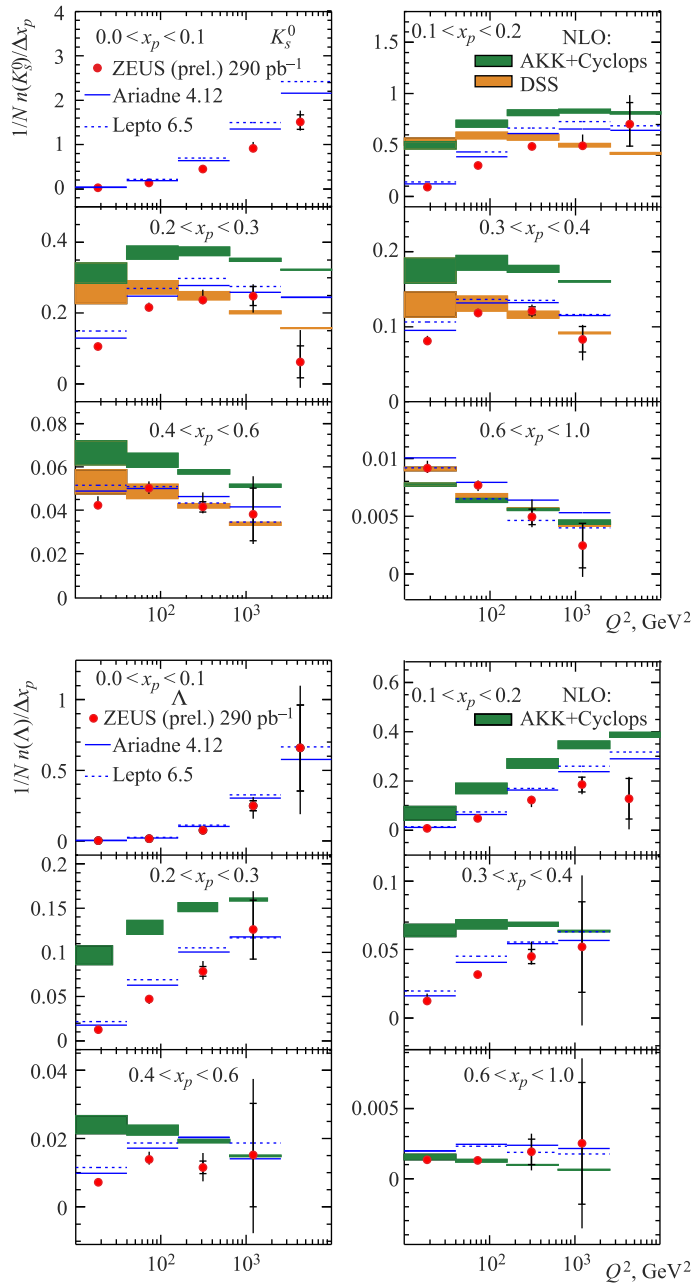


Fig. 6. Scaled momentum distributions for  $K_s^0$  and  $\Lambda$  vs.  $Q^2$  in different regions of  $x_p$

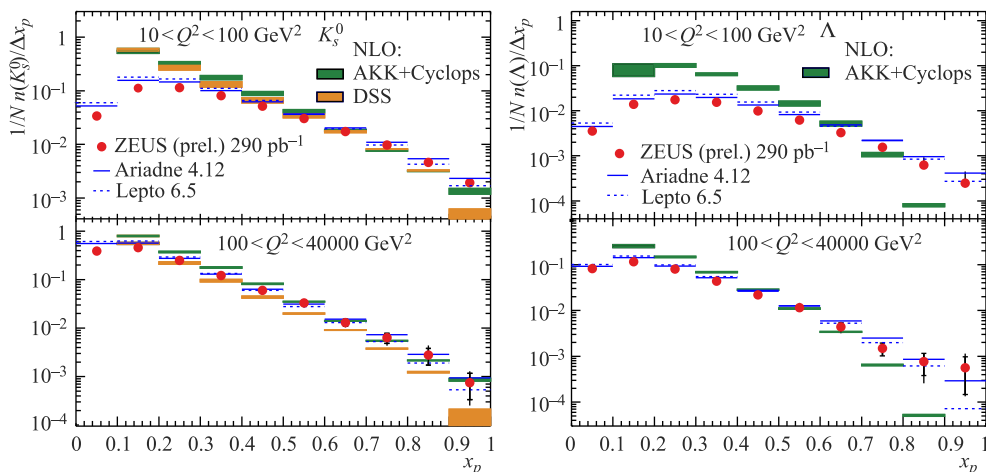


Fig. 7. Scaled momentum distributions for  $K_s^0$  and  $\Lambda$  vs.  $x_p$  in different regions of  $Q^2$

CDM and MEPS LO QCD calculations including hadron-mass effects reproduce the trends of the  $K_s^0$  and  $\Lambda$  measured distributions as functions of  $Q^2$  and the scaled momentum variable reasonably in full phase space. Whereas QCD NLO predictions describe adequately only high- $x_p$  region.

#### REFERENCES

1. Dokshitzer Y. L., Fadin V. S., Khoze V. A. // Phys. Lett. B. 1982. V. 115. P. 242.
2. Azimov Y. I. et al. // Z. Phys. C. 1985. V. 27. P. 65.
3. Abramowicz H. et al. (ZEUS Collab.) DESY-09-229. 2009; JHEP. 2010. V. 2010, No. 6. P. 009.
4. Breitter M. et al. (ZEUS Collab.) // Z. Phys. C. 1995. V. 67. P. 93;  
Breitweg J. et al. (ZEUS Collab.) // Phys. Lett. B. 1997. V. 414. P. 428;  
Breitweg J. et al. (ZEUS Collab.) // Eur. Phys. J. C. 1999. V. 11. P. 251.
5. Aaron F. D. et al. (H1 Collab.) // Phys. Lett. B. 2007. V. 654. P. 148.
6. Petersen A. et al. (MARK II Collab.) // Phys. Rev. D. 1988. V. 37. P. 1.
7. Braunschweig W. et al. (TASSO Collab.) // Z. Phys. C. 1990. V. 47. P. 187.
8. Li Y. K. et al. (AMY Collab.) // Phys. Rev. D. 1990. V. 41. P. 2675.
9. Abreu P. et al. (DELPHI Collab.) // Phys. Lett. B. 1993. V. 311. P. 408.
10. Lonnblad L. // Comp. Phys. Commun. 1992. V. 71. P. 15.
11. Ingelman G., Edin A., Rathsman J. // Comp. Phys. Commun. 1997. V. 101. P. 108.
12. Kretzer S. // Phys. Rev. D. 2000. V. 62. P. 054001.
13. Kniehl B. A., Kramer G., Potter B. // Phys. Rev. Lett. 2000. V. 85. P. 5288.
14. Albino S., Kniehl B. A., Kramer G. // Nucl. Phys. B. 2005. V. 725. P. 181;  
Albino S. et al. // Nucl. Phys. B. 2008. V. 803. P. 42.
15. De Florian D., Sassot R., Stratmann M. // Phys. Rev. D. 2007. V. 75. P. 114010;  
De Florian D., Sassot R., Stratmann M. // Ibid. V. 76. P. 074033.
16. Chekanov S. et al. (ZEUS Collab.) DESY-09-059. 2009; JHEP. 2009. V. 2009, No. 8. P. 077.
17. Acosta D. et al. (CDF Collab.) // Phys. Rev. D. 2003. V. 68. P. 012003.
18. Akrawy M. Z. et al. (OPAL Collab.) // Phys. Lett. B. 1990. V. 247. P. 617.
19. Adeva B. et al. (L3 Collab.) // Phys. Lett. B. 1991. V. 259. P. 199.
20. ZEUS Collab. ZEUS-prel-10-047. 2010.